

Layer-by-layer Adhesion of Hydrogels for Constructing Heterogeneous Microfluidic Chips

Chong Shen¹, Yingjun Li¹, Wenqi She¹, and Qin Meng¹

¹Zhejiang University

May 27, 2023

Abstract

Hydrogel-based microfluidics offer an *in vivo*-relevant micro-environments for construction of organs-on-chips. However, the fabrication of heterogeneous microchannels using hydrogels is challenging and fails to mimic the complex structures of organs *in vivo*. Here we present a new methodology called “layer-by-layer adhesion” for the construction of complex microfluidic chips. A hydrosoluble and photo-crosslinkable adhesive, chitosan methacryloyl (CS-MA), was used to stitch various hydrogels together layer-by-layer to form perfusable microchannels. Our results show that CS-MA can bond different types of hydrogels with adhesion energy ranging from 1.2-140 N/m. Using the layer-by-layer adhesion approach, we constructed heterogeneous hydrogel-based microchannels with various morphologies of snail, spiral, vascular-like, and bilayer. Based on this methodology, liver-on-a-chip was established by entrapping hepatic cells inside a biocompatible Gel-MA layer and covering it with the perfusable microchannels in tough F127-DA layer. The “layer-by-layer adhesion” provides a facile and cytocompatible approach for engineering user-defined hydrogel-based chips potentially for organs-on-chips.

Layer-by-layer Adhesion of Hydrogels for Constructing Heterogeneous Microfluidic Chips

Chong Shen, Yingjun Li, Wenqi She, Qin Meng *

Key Laboratory of Biomass Chemical Engineering (Education Ministry), College of Chemical and Biological Engineering, Zhejiang University, Hangzhou 310027, China.

*Correspondence to: Dr. Qin Meng, College of Chemical and Biological Engineering, Zhejiang University, 38 Zheda Road, Hangzhou, Zhejiang 310027, P.R. China. mengq@zju.edu.cn

Abstract

Hydrogel-based microfluidics offer an *in vivo* -relevant micro-environments for construction of organs-on-chips. However, the fabrication of heterogeneous microchannels using hydrogels is challenging and fails to mimic the complex structures of organs *in vivo* . Here we present a new methodology called “layer-by-layer adhesion” for the construction of complex microfluidic chips. A hydrosoluble and photo-crosslinkable adhesive, chitosan methacryloyl (CS-MA), was used to stitch various hydrogels together layer-by-layer to form perfusable microchannels. Our results show that CS-MA can bond different types of hydrogels with adhesion energy ranging from 1.2-140 N/m. Using the layer-by-layer adhesion approach, we constructed heterogeneous hydrogel-based microchannels with various morphologies of snail, spiral, vascular-like, and bilayer. Based on this methodology, liver-on-a-chip was established by entrapping hepatic cells inside a biocompatible Gel-MA layer and covering it with the perfusable microchannels in tough F127-DA layer.

The “layer-by-layer adhesion” provides a facile and cytocompatible approach for engineering user-defined hydrogel-based chips potentially for organs-on-chips.

Keywords: Hydrogel microfluidic; layer-by-layer; adhesion; sacrificial template; organ-on-a-chip

1. Introduction

Microfluidic chips have revolutionized fluidic manipulation and control at small volumes, finding applications in fields such as diseases diagnosis and cell cultures¹⁻³. Hydrogels, as the backbone of microfluidics, offer advantages over materials such as PDMS or glass due to their biological relevance on biocompatibility, physical stiffness, degradation and mass transport properties^{4,5}. These ideal features make them promising for applications in tissue engineering⁶, biomedical research^{7,8}, and food industry^{9,10}.

Nevertheless, constructing heterogeneous architectures inside hydrogels remains a challenge¹¹, which limits their potential for mimicking the complex and multilayer structures of organs *in vivo*⁵. Sacrificial templates are most commonly used to construct structures inside hydrogel-based microfluidics⁶, where a 3D degradable template is first encapsulated into the hydrogel and then removed to obtain fluidic channels (Figure 1A). However, the sacrificial templates, usually comprised of soft materials such as sodium alginate¹² and gelatin⁶, are mechanically weak and easy to distort during fabrication. Thus, the formed channels are often simple, inaccurate and deviated away from their designed morphology. Moreover, the chips integrally casted by homogeneous material lack the possibility to design multilayers with different materials, making it impossible to mimic the heterogeneous organs *in vivo*^{13,14}. Similarly, other hydrogel-based microfluidic preparation techniques, such as 3D printing¹⁵, light-controlled degradation¹⁶, and direct writing¹⁷, also failed to construct heterogeneous and accurate structures in hydrogels due to complications in handling, poor in resolution or restriction to specific materials.

Figure 1

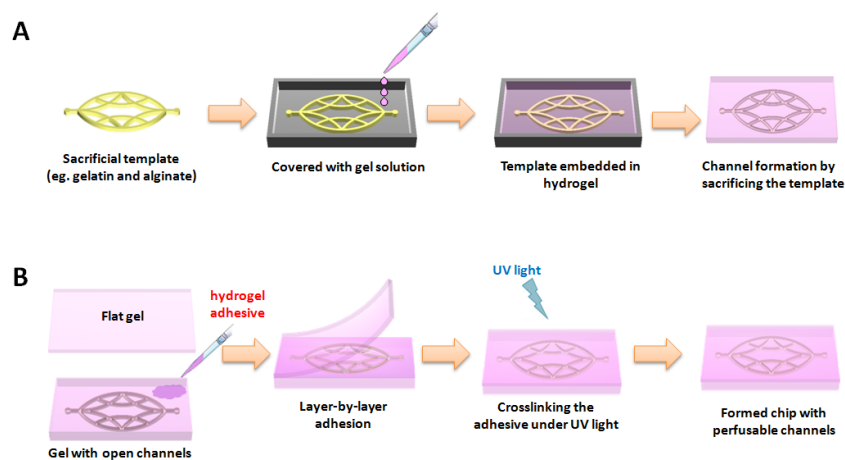


Figure 1 Schematic diagram showing the fabrication of hydrogel-based chip *via* sacrificial templates (A) and layer-by-layer adhesion (B).

To address these limitations, a new and simple strategy of “layer-by-layer adhesion” has been proposed to construct hydrogel-based microfluidics with accurate 3D microchannels and hybrid materials (Figure 1B).

The approach involves preparing predefined microgrooves on the hydrogel surface using soft lithography techniques¹⁸ and bonding other hydrogels layer-by-layer *via* an adhesive. By sealing two or more hydrogel layers, closed and perfusable microchannels are formed inside the chip. This approach is simple and allows for the assembly of various materials into a single chip, greatly improving its designability. The choice of adhesive is critical for this new concept. Commercial glues are unsuitable due to their fragility, toxicity and incompatibility with the wet surfaces of hydrogels^{11,19}. To address this issue, this paper synthesizes a wet-surface adhesive based on the biopolymer chitosan²⁰. To improve the solubility and stability of native chitosan, a hydrosoluble and UV-crosslinkable chitosan methacryloyl (CS-MA) will be prepared at physiological pH *via* N-acylation reaction. Finally, the CS-MA adhesive will be used to stitch various hydrogel layers and construct liver-on-a-chip to compare with that made using sacrificial templates.

2. Materials and Methods

2.1 Experimental procedure of hydrogel adhesion

CS-MA was synthesized according to the previously reported method²¹. Briefly, 1.2 ml methacrylic anhydride was added slowly to 1% (w/v) chitosan (CS, MW 30,000 Da) in acetic acid solution (400 ml) and reacted for 4 h at 50 °C. The solution was neutralized by 10% (w/v) sodium bicarbonate solution and dialyzed against deionized water for 3 days before lyophilization. The CS-MA was characterized by ¹H NMR with D₂O as solvent and FTIR by the KBr pellets method. The CS-MA adhesive solution was prepared by dissolving the CS-MA powder at 4 wt% and VA-086 at 0.2 wt% into PBS solution at pH 7.

Five representative hydrogels in tissue engineering were prepared according to the methods outlined in the Supporting Information. The prepared CS-MA solution was directly and uniformly applied to the surface of two pieces of hydrogels. After 5 to 120 min of incubation, one piece of hydrogel was placed on top of the other, and the two pieces were integrated *via* slight compression using a glass slide for 5 to 120 min. Subsequently, the two pieces of hydrogels were exposed to ultraviolet (UV) light for 30 s to crosslink the CS-MA monomer.

2.2 Characterization of bonded hydrogels

The adhesion energy of hydrogels was measured by T-peeling tests (Supporting Information), while the mechanical properties were measured by elongation and compressive testing using an Instron Series IX Automated Materials Testing System (Zwick/Roell Z020)²². Moreover, the bonded surface was observed using a field-emission scanning electron microscopy (FE-SEM). To prepare the samples, the hydrogels were cut into slices perpendicular to the bonding interface, and the slices were then transferred to a vacuum freeze dryer for 24 h of dehydration and were sputter-coated with Pt before SEM observation.

2.3 Construction of hydrogel-based microfluidic chips

Firstly, a set of molds with diverse forms of microgroove forms were designed with Solidworks software and manufactured through 3D printing with white resin (Deed 3D Corporation, Guangzhou, China). Next, PDMS stamps were prepared by casting prepolymerized PDMS on the 3D printed molds and cured at 80°C for 3 h. After removing the 3D printed mold, the monomer solution for different hydrogels was poured onto the PDMS stamp and polymerized using the methods described in Supporting Information. After discarding the PDMS stamp, the hydrogel layer with open channels was coated with the CS-MA solution for 60 min, and the residue CS-MA solution on the surfaces was subsequently removed before covered by a flat gel sheet for 60 min and UV irradiation for 10 min. For perfusion, silicone tubes (1 mm × 1.5 mm) connected with stainless steel tubes were taped to the access holes on the chip and a red dye of Rho B was injected into channels for dynamic perfusion.

2.4 Fabrication of liver-on-a-chip

Liver hepatocellular carcinoma HepG2 were from American Type Culture Collection (ATCC) and cultured in DMEM with 10% FBS. Human umbilical vein endothelial cells (HUVECs) were purchased from Lonza (Walkersville, MD, USA) and cultured in EGM-2 medium supplemented with 100 U/ml penicillin and 100 mg/L streptomycin at 37°C and 5% CO₂.

To encapsulate the HepG2 cells inside the hydrogel, 10 wt% Gel-MA was dissolved in phosphate buffer solution (PBS) at pH 7.4 and then autoclaved at 121 °C for 30 min. The HepG2 cell suspension was mixed with the Gel-MA solution which was supplemented with 0.2 wt% VA-086 to obtain a final density at 10⁶ cells/ml. The cell-laden hydrogel was formed by pouring the solution into a sterilized PDMS stamp, followed by a 30 s exposure to a UV light at 395 nm.

The Gel-MA and F127-DA sheets were coated with the CS-MA solution for 30 min in a sterilized glass mold. Then, the F127-DA layer was placed onto the Gel-MA layer for a UV light exposure at 395 nm for 30 s to assemble the chip. The hydrogel chip was then taken out and incubated in DMEM medium with 10% FBS for 48 h at 37°C. Next, the HUVECs suspension in EGM-2 medium at a density of 2×10⁵ cells/ml was injected into the channel of the chip. The chip was perfused by EGM-2 medium for another 2 days culture.

2.5 Cell activity analysis and immunostaining

The cell viability of the chip was tested using a cell LIVE/DEAD assay kit. After being rinsed with PBS, the chips were stained with Calcein AM and PI solution at concentrations of 10 μM and 4 μM, respectively. After incubation with the Calcein AM/PI solution for 40 min, the chips were washed with PBS and observed under a fluorescence microscope (OLYMPUS Ix70). Moreover, the MTT reduction was used to evaluate the cell viability of HepG2 and HUVECs in the chips. Briefly, the chips were rinsed by PBS before being immersed in 5 ml of the MTT-PBS at 1.15 mg/ml. After being incubated at 37°C for 3 h, the chips were washed by PBS and then added by 5 ml of acidified isopropanol. After agitation for 3 h, the extraction was measured at absorbance of 570 nm on a spectrophotometer.

The chips were immunostained by VEGF and MRP-2 to show the HUVECs and HepG2 cells respectively. Briefly, the chip was blocked using 1.5% fish skin gelatin in PBS containing 0.025% Trion-X 100 for 90 min at room temperature and incubated with 1:100 diluted primary antibodies (Rabbit Anti-VEGF and Mouse Anti-MRP-2) overnight at 4°C. After washing with PBS and incubating with secondary antibody (DyLight 488-Goat Anti Rabbit IgG and DyLight 594-Goat Anti Mouse IgG) for 1 h at room temperature, the sample was stained by DAPI for 5 min and imaged by a fluorescent microscope (OLYMPUS Ix70).

2.6 Statistical analysis

All data from cell experiments were analyzed by means ± SD from three independent experiments. Comparisons between multiple groups were performed with the ANOVA test by SPSS, or results from two different groups were tested with the unpaired Student t-test. P-values less than 0.05 were considered statistically significant.

3. Results and discussion

3.1 Synthesis of hydrosoluble and photo-crosslinkable CS-MA

Natural CS cannot be dissolved in a neutral pH solution due to the hydrogen bonds between its amino and hydroxyl groups²¹. When the pH of CS solution (4 wt% CS dissolved in 0.1% acetic acid) was adjusted to 7, the pH-responsive CS precipitated from the solution (Figure 2A). However, the pH-sensitivity of CS was significantly attenuated after grafting of acrylate groups for the reduced hydrogen bonds, resulting in the formation of a hydrosoluble CS-MA in solution at pH 7 (Figure 2A).

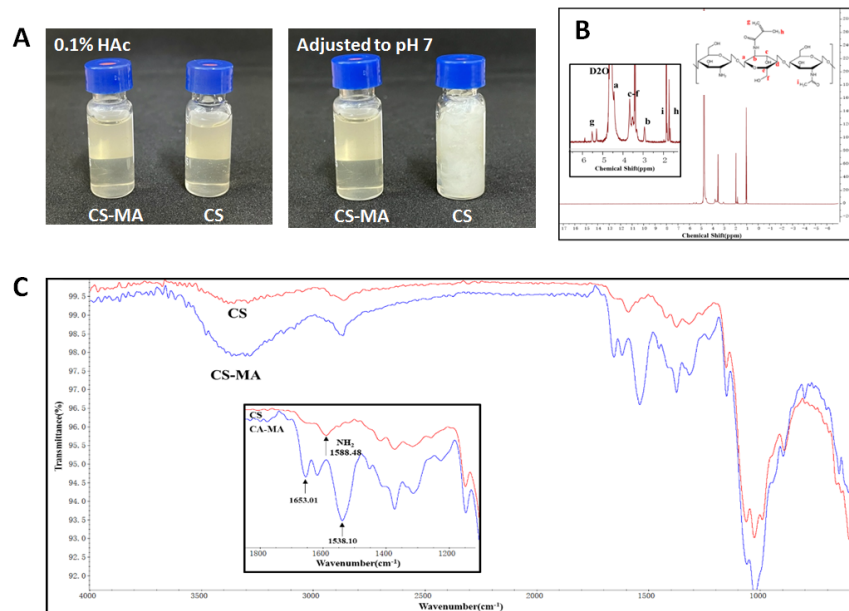


Figure 2 Characterization of hydrosoluble and photo-crosslinkable CS-MA. (A) Solubility of CS and CS-MA in acid and neutral solution. (B) ¹H NMR spectrum of CS-MA. (C) FTIR spectrum of CS and CS-MA.

The chemical structure of CS-MA was confirmed through the analysis of its ¹H NMR spectrum (Figure 2B). The signals at 5.40 and 5.62 ppm (g) indicated the presence of vinyl protons. The signals at 4.68 (a), 2.93 (b) and 3.42-3.76 ppm (c-f) were attributed to the protons of the glucose ring, while the peaks at 1.94 ppm (i) and 1.81 ppm (h) represented the methyl protons of N-acetylglucosamine and methacrylic anhydride residues. In contrast, CS did not exhibit any signal at 5.5-6.0 ppm^{23,24}. Furthermore, the successful reaction of CS with methacrylic anhydride was confirmed through FTIR spectrum (Figure 2C). The appearance of new peaks at 1653 and 1538 cm⁻¹ indicated the presence of C=O stretching and N-H deformation/C-N stretching. The peak at 1588 cm⁻¹, corresponding to -NH₂, disappeared due to its involvement in the newly formed amide bonds²¹.

3.2 CS-MA well stitched various hydrogels

The hydrogel stitching comprised of two main steps, coating and integration (Figure 3A), prior to the CS-MA polymerization, while the T-peeling test process was illustrated in Figure S1. The optimal coating and integrative time for the two PAAM sheets were determined to be 120 and 30 min, respectively (Figure 3B and 3C). Following the same experimental procedure, the maximum adhesion energy was obtained for the four types of hydrogels when bonded to each other (Figure 3D). The PAAM layer adhering to another PAAM exhibited the highest adhesion energy of 140 N/m, while the adhesion energy between the PAAM hydrogel and Gel-MA was the lowest at 3.2 N/m (Figure 3D). The peeling test revealed that the hydrogel themselves cracked before the cohesive failure of the bonded interface (Supplementary Movie 1). As Gel-MA had the weakest mechanical strength among the four hydrogels, the Gel-MA sheet broken before the adhesion failure, resulting in the low adhesion energy. Hence, the adhesion energy at the interface of two hydrogels was mainly determined by their mechanical strength rather than the bonding of CS-MA.

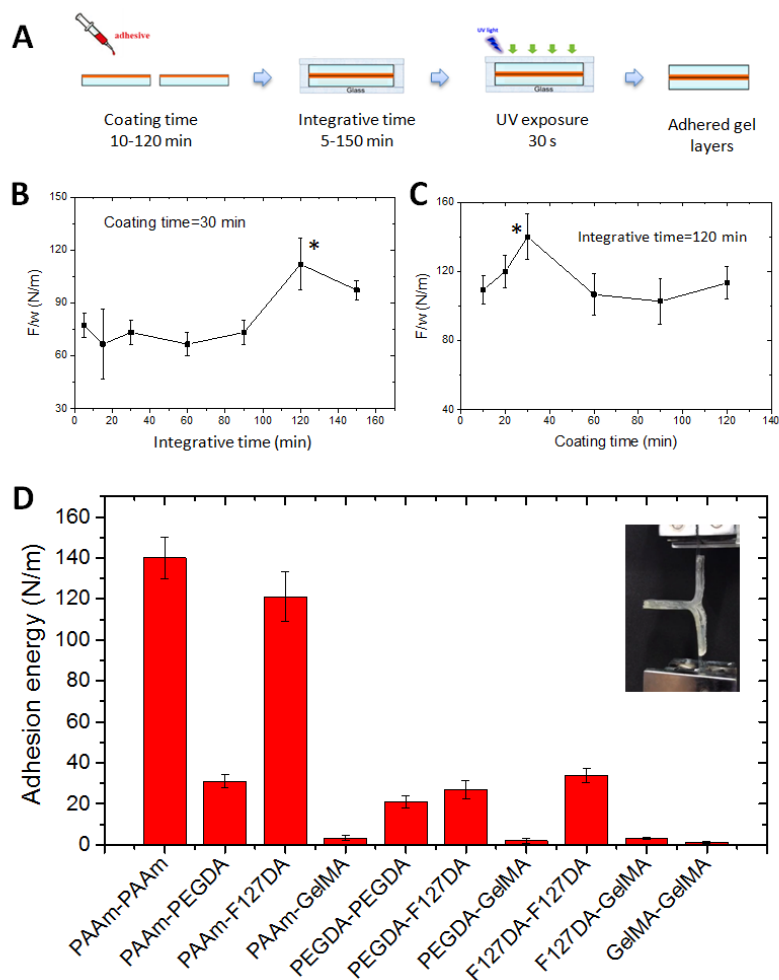


Figure 3 Bonding strength of CS-MA to four types of hydrogels. (A) Process of hydrogel adhesion. (B-C) Adhesion energy (Force/width, F/w) of PAAm hydrogels varies with the coating and integrative time. * $p < 0.05$ when compared with other groups. (D) Maximum adhesion energy of various hydrogels at optimized coating and integrative time. Small image is the T-peeling test of PAAm hydrogels.

To further confirm the stitching stability under deformation, the adhered PAAm hydrogels were stretched and compressed on an automated materials testing system. During the stretching, the hydrogels were broken before debonding (Figure S2), indicating strong adhesion. Moreover, the intact and stitched PAAm hydrogels withstood similar compressive stress of > 2.7 MPa (Figure S2), indicating that the mechanical strength was not weakened after suture.

Autoclaving is a commonly used and effective sterilization method but may sometimes damage the polymer network by inducing phase separation and aggregation²⁵. Therefore, the resistance of hydrogels to autoclaving is a crucial concern for their applications in cell culture and tissue engineering. To examine the alteration of adhesion energy before and after autoclaving, the adhered PAAm hydrogels were sterilized at 121°C for 30 min. As shown in Figure S3, the adhesion energy of PAAm hydrogels was not impaired by autoclaving, although the mechanical strength was reduced due to swelling. Since CS is known as a thermal stable polymer²⁶, the stable adhesion by CS-MA is likely due to the covalently crosslinked CS chains that were modified by N-acylation reaction²¹. In contrast, the adhesion by other hydrogel adhesives, such as

pristine chitosan²⁷ and poly(acrylic acid)/Fe³⁺+²⁸, was unstable under varying conditions due to the ionic bonds of adhesive chains, which is unsuitable for sealing hydrogel-based microfluidic chips.

3.3 Mechanism of the adhesion between hydrogels *via* CS-MA

The strong adhesion between the adhesive chains and the hydrogels' network could be attributed to their topological entanglement¹¹. To investigate the interface of bonded PAAm hydrogels, SEM was used and it revealed a dense interfacial zone with a thickness of 30-50 μm between two sheets after stitching (Figure 4A). This suggested that the CS-MA diffused into the porous hydrogels and was crosslinked inside the pores. In contrast, hydrogels without CS-MA treatment showed a clear interface (Figure 4B) and could be easily peeled along the interface, resulting in a low adhesion energy of ~ 1 N/m. The CS-MA diffusion into hydrogel was also visibly monitored using fluorescent FITC labeled CS-MA (Figure 4C and 4D). Since the CS-MA has lost the pH responsibility of CS (Figure 2A), it could diffuse into the hydrogel freely. Consequently, the CS-MA rich layer gradually thickened during coating but diffused away from the interface over the integrative time. The well permeation of CS-MA might be able to interlock the two hydrogels after polymerization and ensure strong adhesion²⁷. This explained why extending the coating time facilitated adhesion (Figure 3).

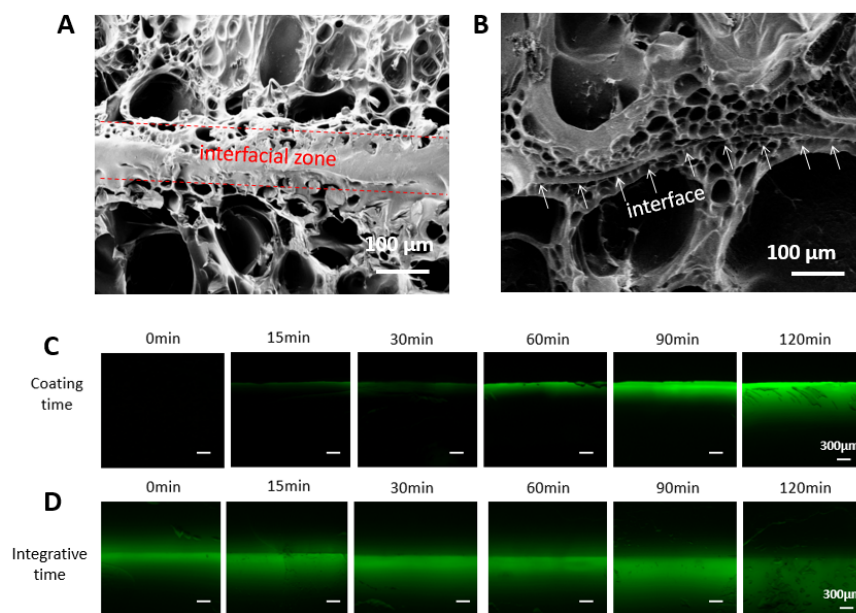


Figure 4 Microstructure of stitching interface. SEM images of the interfaces of two PAAm hydrogels with (A) or without (B) stitching. Scale bar=100 μm . Sequence of fluorescent microscopic images show that the FITC labeled CS-MA diffuses from the interface of PAAm hydrogels in coating (C) and integrative (D) periods. Scale bar=300 μm .

3.4 Construction of 3D architectures and microfluidic chips *via* layer-by-layer adhesion

Using layer-by-layer adhesion, various architectures can be constructed from different hydrogels. Here we provide some examples that are unable to be fabricated by sacrificial templates. Firstly, we obtained a 3D architecture by stitching PAAm and F127-DA hydrogel strips with CS-MA. As shown in Figure 5A, the strips were superimposed on each other and after stitching, the strips well bonded together, which can be pulled without detachment (Supplementary Movie 2). Furthermore, a microfluidic chip was assembled by three hydrogels of PAAm, F127-DA and PEG-DA, providing an inner vascular-like channel (Figure 5B). The

hydrogel chip endured a sharp twist without cracking (Supplementary Movie 3), indicating strong adhesion among the hydrogels.

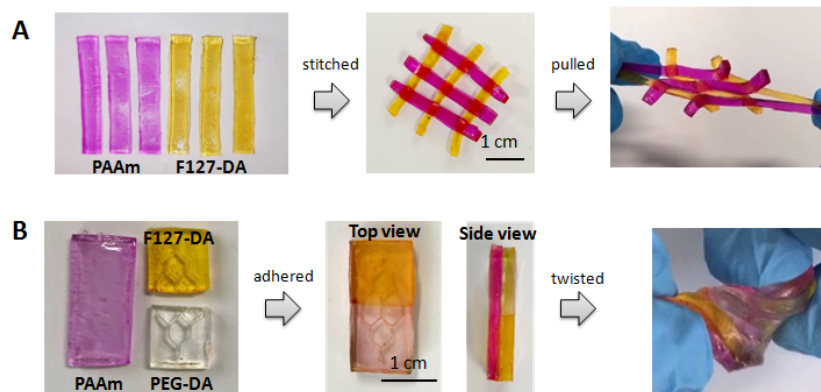


Figure 5 Construction of 3D architectures *via* layer-by-layer adhesion. (A) 3D architecture constitutes hydrogel strips. (B) The chip with vascular-like microchannels comprises three parts of hydrogels.

We also used this method to construct perfusable microfluidic chips with complex channels. After sealing by CS-MA, the F127-DA/PAAm and PEG-DA/PAAm chips were obtained with corresponding microchannels (Figure 6A and 6B). By perfusion of red Rho B solution, the microchannels revealed with snail and spiral morphology (Supplementary Movie 4). These complex channels with sharp turns still performed at high resolution, which was better than those made by sacrificial templates^{6,12} and 3D printing¹⁵. Another example was a bilayer chip that was commonly used for coculture of cells. As shown in Figure 6C, a PAAm film was stitched between two F127-DA hydrogels, where the bilayer microchannels could be perfused individually.

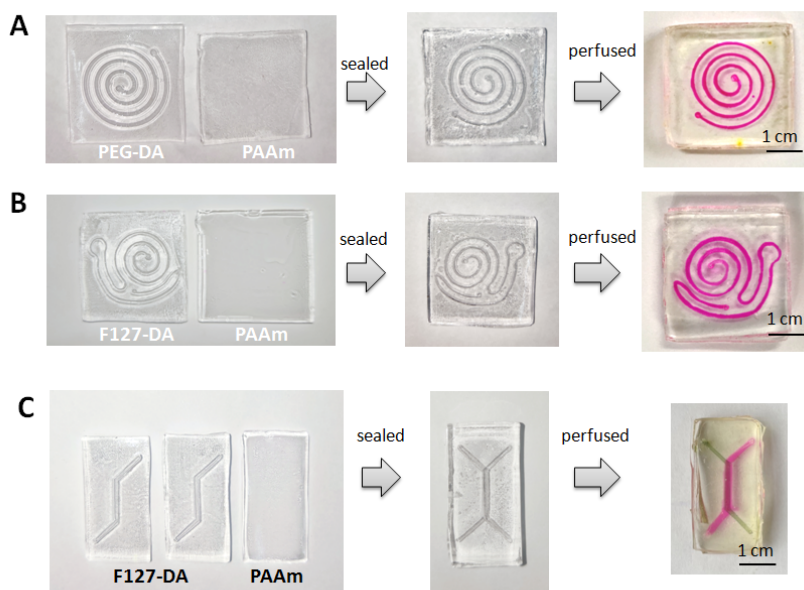


Figure 6 Construction of perfusable microfluidic chips *via* layer-by-layer adhesion. (A) Perfusable microfluidic

chip with spiral pattern. (B) Perfusable microfluidic chip with snail pattern. (C) Bilayer chip for coculture of cells. Scale bar=1 cm.

3.5 Application of layer-by-layer adhered microfluidic as liver-on-a-chip

As a common practice with microfluidics, liver-on-a-chip was constructed to mimic the hepatic structures. The hydrogel microfluidic chip is typically constructed using Gel-MA, a photo-crosslinkable polymer²⁹. However, Gel-MA is mechanically weak and cannot withstand perfusing-induced shear stress. To address this issue, we encapsulated the HepG2 cells in Gel-MA and stitched it onto a tough F127-DA sheet to reinforce the Gel-MA layer (Figure 7A). HUVECs were seeded on the surface of the channel for perfusion culture (Figure 7A).

The key step in the construction was the adhesion of the cell-laden Gel-MA hydrogel to the F127-DA sheet. The neutral CS-MA adhesive used was well-tolerated by HepG2 cells (Figure S4). To minimize the injury during stitching, a short UV exposure of 30 s with a flashlight was applied for the CS-MA photo-crosslinking in the presence of VA-086, since long-wave UV light (395 nm) triggered low toxicity to cells³⁰. After 2 days of perfusing culture, cell viability was assessed using Calcein AM/PI staining, which detects living and dead cells^{29,31}. Based on fluorescent images, most of cells (both HepG2 and HUVECs) were alive (stained green, Figure 7B), with only a very small amount of dead cells (stained red, Figure 7C). The spread cells in the channel zone (shown by the white line in Figure 7B to 7D) were likely HUVECs, while the round cells and aggregates located in the entire chip would be HepG2 cells, as the encapsulated HepG2 cells possibly grew or migrated to aggregates within 4 days of culture. Quantitative analysis showed that encapsulation decreased the viability of HepG2 cells to 75%, but it increased to over 80% after 1 day's incubation due to the proliferation of living cells (Figure 7E). Moreover, the seeded HUVECs were mostly alive within 2 days of perfusion culture (Figure 7E).

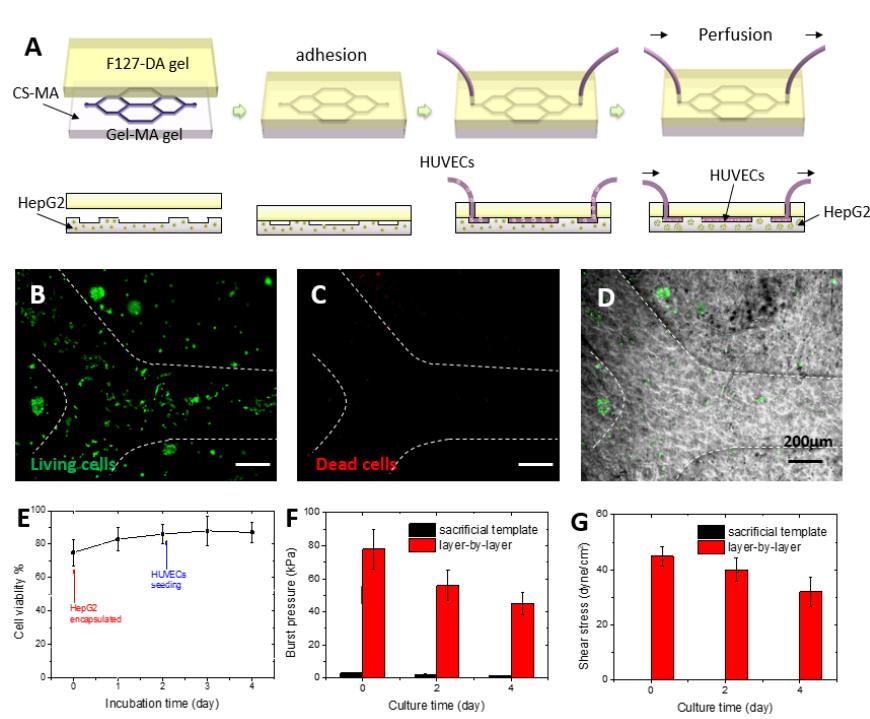


Figure 7 Cell viability and morphology in liver-on-a-chip. (A) Schematic of cell encapsulation and seeding. (B-D) Representative images showing living cells (green: Calcein AM) and dead cells (red: PI) at Day 4. Scale bar=200 μ m. (E) Cell viability at Day 0 to Day 4. (F) Comparison of burst pressure of the chips made

by layer-by-layer adhesion and sacrificial template. (G) Maximum shear stress that the chips were able to endure.

In previous study, poly-L-lysine has been used as an electrostatic glue to seal the hydrogel-based chips³². However, this method provided weak adhesion with fluid leakage occurring at applied pressures higher than 3 kPa, providing an extremely low shear stress of approximately 0.1 dyne/cm². To compare the perfusion tolerance of chips constructed by different methods, liver-on-a-chip with the same channel morphology was constructed by Gel-MA hydrogel and alginate sacrificial template. As shown in Figure 7F, the chip made by layer-by-layer adhesion showed the high burst pressure of >40 kPa during the culture, due to the strong support provided by the tough F127-DA layer³³. In contrast, the Gel-MA chip made by sacrificial template was brittle and weak, and was easily broken by an extremely low pressure of 3 kPa. Consistently, the assembled chip shown in Figure 7A was able to withstand flow-induced shear stress of >45 dyne/cm², which is in the range of physiological values of 1-50 dyne/cm² in human blood vessels³⁴. However, the Gel-MA chip made by sacrificial template could only tolerate a very low shear stress of 0.1-0.2 dyne/cm², thus limiting its applications in perfusing culture. As the accurate mimicking of mechanical microenvironments is essential in construction of organs-on-chips³⁵, layer-by-layer adhesion performs better than the use of sacrificial templates.

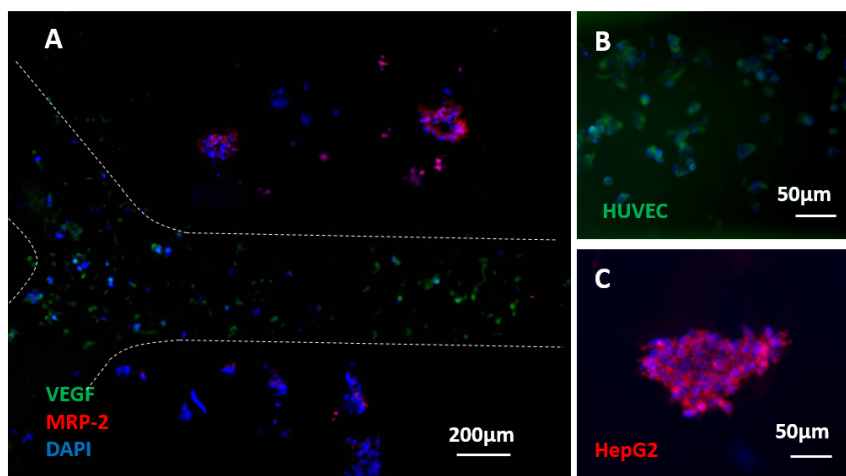


Figure 8 Identification of HepG2 cells and HUVECs by immunostaining. (A) HUVECs (green, stained with VEGF) attached on the surface of channel. (B) HepG2 cells (red, stained with MRP-2) located in Gel-MA hydrogel. Nuclei were stained blue by DAPI. White line was the borderline of microchannel.

To visually depict the cellular organization within the chip, we immunostained MRP-2 and VEGF to identify HepG2 cells and HUVECs, respectively. MRP-2 is specifically expressed in hepatic cells that mediates the drug transportation³⁶, while VEGF is secreted by HUVECs but not HepG2 cells to regulate the endothelial angiogenesis and permeability³⁷. As shown in Figure 8A, VEGF-positive HUVECs were located in the channel zone, while the MRP-2 positive HepG2 cells were dispersed inside Gel-MA hydrogel. Zoom-in images showed the specific expression of VEGF (green, Figure 8B) and MRP-2 (red, Figure 8C) by HUVECs and HepG2 cells, respectively. The HepG2 cells formed irregular aggregates in Gel-MA hydrogel (Figure 8C), consistent with previous reports³⁸.

While the above example did not cover all the possible applications of layer-by-layer adhesion in constructing hydrogel-based microfluidics, it presented a novel and straightforward concept for fabricating complex and precise 3D architectures. Moreover, another example was shown in Figure S5, where a bilayer chip was constructed for coculture of HepG2 cells and fibroblasts. To replicate the physiology of organs, current

biofabrication techniques require the spatially-precise organization of cells and extracellular matrix, mimicking physical cues *in vivo* such as chemical components, topography, stiffness and shear stress². Hence, the layer-by-layer adhesion could aid in the rational design of *in vivo*-like tissues, as multilayered hydrogels facilitate the mimicking of chemical and structural properties of extracellular matrix *in vivo*. This paper demonstrated the construction of liver-on-a-chip with vascular structure by organizing liver and endothelial cells in the appropriate positions (Figure 7), well mimicking the vasculature and sustaining cellular activity in the liver³⁹. Similarly, the layer-by-layer adhesion could also benefit the design of other organs-on-chips such as skin consisting of various layers with different extracellular matrix and cells^{40,41}.

4. Conclusion

We have introduced a new method called “layer-by-layer adhesion” for constructing hydrogel-based microfluidic chips. Four types of hydrogels were well stitched together using the adhesive properties of CS-MA, which exhibited adhesion energy of 1.2-140 N/m. The CS-MA diffused into the hydrogels and then crosslinked at the interface of two hydrogels to create a density zone. Such adhesion maintained good stability even after autoclaving, stretching and twisting. This method allowed for the assembly of perfusable hydrogels with snail, spiral, vascular-like and bilayer microchannels with high resolution. As an example of application, we used this method to construct liver-on-a-chip based on Gel-MA/F127-DA layers and coculture of HepG2 cells with HUVECs. Our method of layer-by-layer adhesion offers a new way to design 3D architectures in hydrogels and construct microfluidic organs-on-chips *in vitro*.

5. Data availability statement

The data that supports the findings of this study are available in the supplementary material of this article.

6. Conflicts of interest

There are no conflicts of interest to declare.

7. Acknowledgement

We gratefully acknowledge the financial support of this study by NSFC (National Natural Science Foundation of China, No 22078287 and 21978257).

8. References

1. Sun WJ, Luo ZM, Lee J, et al. Organ-on-a-Chip for Cancer and Immune Organs Modeling. *Advanced Healthcare Materials*. Feb 21 2019;8(4).
2. Sontheimer-Phelps A, Hassell BA, Ingber DE. Modelling cancer in microfluidic human organs-on-chips. *Nat Rev Cancer*. Feb 2019;19(2):65-81.
3. Rothbauer M, Zirath H, Ertl P. Recent advances in microfluidic technologies for cell-to-cell interaction studies. *Lab on a Chip*. Jan 21 2018;18(2):249-270.
4. Huang GY, Zhou LH, Zhang QC, et al. Microfluidic hydrogels for tissue engineering. *Biofabrication*. Mar 2011;3(1):012001.
5. Zhang X, Li L, Luo C. Gel integration for microfluidic applications. *Lab Chip*. May 21 2016;16(10):1757-1776.
6. Zhao S, Chen Y, Partlow BP, et al. Bio-functionalized silk hydrogel microfluidic systems. *Biomaterials*. Jul 2016;93:60-70.
7. Paguirigan A, Beebe DJ. Gelatin based microfluidic devices for cell culture. *Lab Chip*. Mar 2006;6(3):407-413.

8. Gjorevski N, Lutolf MP. Synthesis and characterization of well-defined hydrogel matrices and their application to intestinal stem cell and organoid culture. *Nat Protoc.* Nov 2017;12(11):2263-2274.
9. Feng YM, Lee Y. Microfluidic assembly of food-grade delivery systems: Toward functional delivery structure design. *Trends Food Sci Tech.* Apr 2019;86:465-478.
10. Kim YH, Kim DJ, Lee S, Kim DH, Park SG, Kim SH. Microfluidic Designing Microgels Containing Highly Concentrated Gold Nanoparticles for SERS Analysis of Complex Fluids. *Small.* Dec 2019;15(52).
11. Yang JW, Bai RB, Chen BH, Suo ZG. Hydrogel Adhesion: A Supramolecular Synergy of Chemistry, Topology, and Mechanics. *Advanced Functional Materials.* Jan 2020;30(2).
12. Wang XY, Jin ZH, Gan BW, Lv SW, Xie M, Huang WH. Engineering interconnected 3D vascular networks in hydrogels using molded sodium alginate lattice as the sacrificial templatet. *Lab on a Chip.* Aug 7 2014;14(15):2709-2716.
13. Abbott RD, Kaplan DL. Strategies for improving the physiological relevance of human engineered tissues. *Trends Biotechnol.* Jul 2015;33(7):401-407.
14. Lee SH, Sung JH. Organ-on-a-Chip Technology for Reproducing Multiorgan Physiology. *Advanced Healthcare Materials.* Jan 24 2018;7(2).
15. Knowlton S, Yu CH, Ersoy F, Emadi S, Khademhosseini A, Tasoglu S. 3D-printed microfluidic chips with patterned, cell-laden hydrogel constructs. *Biofabrication.* Jun 20 2016;8(2):025019.
16. Lutolf MP. Spotlight on hydrogels. *Nature Materials.* Jun 2009;8(6):451-453.
17. Wu W, Hansen CJ, Aragon AM, Geubelle PH, White SR, Lewis JA. Direct-write assembly of biomimetic microvascular networks for efficient fluid transport. *Soft Matter.* 2010;6(4):739-742.
18. Thomsen AR, Aldrian C, Bronsert P, et al. A deep conical agarose microwell array for adhesion independent three-dimensional cell culture and dynamic volume measurement. *Lab Chip.* Dec 19 2018;18(1):179-189.
19. Yuk H, Varela CE, Nabzdyk CS, et al. Dry double-sided tape for adhesion of wet tissues and devices. *Nature.* Nov 7 2019;575(7781):169-+.
20. Kim IY, Seo SJ, Moon HS, et al. Chitosan and its derivatives for tissue engineering applications. *Biotechnol Adv.* Jan-Feb 2008;26(1):1-21.
21. Li BQ, Wang L, Xu F, et al. Hydrosoluble, UV-crosslinkable and injectable chitosan for patterned cell-laden microgel and rapid transdermal curing hydrogel in vivo. *Acta Biomater.* Aug 2015;22:59-69.
22. Yin HY, Akasaki T, Sun TL, et al. Double network hydrogels from polyelectrolytes: high mechanical strength and excellent anti-biofouling properties. *J Mater Chem B.* 2013;1(30):3685-3693.
23. Qi Z, Xu J, Wang Z, Nie J, Ma G. Preparation and properties of photo-crosslinkable hydrogel based on photopolymerizable chitosan derivative. *International journal of biological macromolecules.* 2013;53(none):144-149.
24. Monier M, Wei Y, Sarhan AA, Ayad DM. Synthesis and characterization of photo-crosslinkable hydrogel membranes based on modified chitosan. *Polymer.* 2010;51(5):1002-1009.
25. Galante R, Pinto TJA, Colaco R, Serro AP. Sterilization of hydrogels for biomedical applications: A review. *J Biomed Mater Res B Appl Biomater.* Aug 2018;106(6):2472-2492.
26. Takei T, Danjo S, Sakoguchi S, et al. Autoclavable physically-crosslinked chitosan cryogel as a wound dressing. *J Biosci Bioeng.* Apr 2018;125(4):490-495.
27. Yang JW, Bai RB, Suo ZG. Topological Adhesion of Wet Materials. *Advanced Materials.* Jun 20 2018;30(25).

28. Gao Y, Wu KL, Suo ZG. Photodetachable Adhesion. *Advanced Materials*. Feb 8 2019;31(6).
29. Zhao X, Lang Q, Yildirimer L, et al. Photocrosslinkable Gelatin Hydrogel for Epidermal Tissue Engineering. *Advanced Healthcare Materials*. Jan 2016;5(1):108-118.
30. Occhetta P, Visone R, Russo L, Cipolla L, Moretti M, Rasponi M. VA-086 methacrylate gelatine photopolymerizable hydrogels: A parametric study for highly biocompatible 3D cell embedding. *Journal of Biomedical Materials Research Part A*. Jun 2015;103(6):2109-2117.
31. Wang ZJ, Kumar H, Tian ZL, et al. Visible Light Photoinitiation of Cell-Adhesive Gelatin Methacryloyl Hydrogels for Stereolithography 3D Bioprinting. *Acs Appl Mater Inter*. Aug 15 2018;10(32):26859-26869.
32. Yajima Y, Yamada M, Yamada E, Iwase M, Seki M. Facile fabrication processes for hydrogel-based microfluidic devices made of natural biopolymers. *Biomicrofluidics*. Mar 2014;8(2):024115.
33. Shen C, Li Y, Wang Y, Meng Q. Non-swelling hydrogel-based microfluidic chips. *Lab Chip*. Dec 7 2019;19(23):3962-3973.
34. Baeyens N, Bandyopadhyay C, Coon BG, Yun S, Schwartz MA. Endothelial fluid shear stress sensing in vascular health and disease. *J Clin Invest*. Mar 1 2016;126(3):821-828.
35. Liu HT, Wang YQ, Cui KL, Guo YQ, Zhang X, Qin JH. Advances in Hydrogels in Organoids and Organs-on-a-Chip. *Advanced Materials*. Dec 13 2019;31(50).
36. Gissen P, Arias IM. Structural and functional hepatocyte polarity and liver disease. *J Hepatol*. Oct 2015;63(4):1023-1037.
37. Apte RS, Chen DS, Ferrara N. VEGF in Signaling and Disease: Beyond Discovery and Development. *Cell*. Mar 7 2019;176(6):1248-1264.
38. Pimentel CR, Ko SK, Caviglia C, et al. Three-dimensional fabrication of thick and densely populated soft constructs with complex and actively perfused channel network. *Acta Biomater*. Jan 2018;65:174-184.
39. Miller JS, Stevens KR, Yang MT, et al. Rapid casting of patterned vascular networks for perfusable engineered three-dimensional tissues. *Nat Mater*. Sep 2012;11(9):768-774.
40. Kim JJ, Ellett F, Thomas CN, et al. A microscale, full-thickness, human skin on a chip assay simulating neutrophil responses to skin infection and antibiotic treatments. *Lab on a Chip*. Sep 21 2019;19(18):3094-3103.
41. Mori N, Morimoto Y, Takeuchi S. Skin integrated with perfusable vascular channels on a chip. *Biomaterials*. Feb 2017;116:48-56.